Material Characterization of Elastomeric Bearing Elements in Wave Energy Converters

R. Duraisamy, K. Andersson

Abstract—**According to the European Council, 75% of the greenhouse emissions are caused by energy production and use. In order to decarbonize the energy sector, more research is focused towards the renewable energy sources. Among the many available resources, wave energy is one of the key resources to consider. As part of the research, KTH is developing a winch based point absorber wave energy converter. The winch consists of a chain link with elastomer bearings wound around a drum. The winding and unwinding motion of chain converts wave motion into electricity. A typical winch based wave energy converter undergoes around 80 million cycles in its lifetime. This calls for a durable system design requiring minimal service and maintenance. With an elastomer bearing, the winding and unwinding of the chain over the drum is realized as deformation of the elastomer thereby eliminating sliding. While the use of elastomer enables an efficient design, it also makes it more challenging due to its highly non-linear and viscoelastic behavior. A constitutive model is necessary to determine material characteristics of an elastomer for different loading conditions. In this work, a systematic design process is outlined and an attempt is made to determine a suitable hyperelastic material model for the elastomer. The study is focused on two materials – silicone and polyurethane. The test samples are compressed and followed by shear in deformation. For material model determination, the test data is curve fit and later verified using finite element method. The material is assumed incompressible.**

Keywords— **constitutive modelling, elastomers, hyperelasticity, material characteristics, renewable energy, viscoelasticity, winch based wave energy converters**

I. Introduction

OCEAN waves are a huge untapped potential source of renewable energy. The estimated capacity of ocean energy around the world is about 2 TW [1]. Initially, the wave energy research started in 1970s during the emerging oil crisis. Due to the recent climate change and the rising levels of global warming, the research in renewable sources of energy is gaining a lot of traction [2, 3].

Among the renewable sources of energy available, ocean energy has higher energy density and efficiency compared to other sources. However, given the challenges that follow with the harsh conditions of the ocean, a significant amount of research is being focused on establishing ocean energy in the current renewable energy market [1]. Some of the main challenges faced when developing wave energy converters are listed below:

High forces and fatigue life: The average energy density of the ocean waves is higher than other renewable sources. During storms, the power levels can reach 50 times higher than average. A durable mechanical structure is required to withhold these high forces during storms. A year of wave energy converter (WEC) at an off shore site induces approximately 4 million load cycles. Moreover, even though the storm load conditions are few, it accumulates to a significant number over the entire service life of a WEC [4].

Marine environment: Due to its harsh environmental conditions, the developing cost of a WEC is high as it is difficult to perform any repairs. In order to keep the maintenance to a minimum, durable mechanical structure and control systems must be developed. Moreover, the WEC must be manufactured with eco-friendly materials and should not harm to the marine eco-system.

Levelized cost of electricity: The cost of energy harvested from the ocean waves must be competitive with other available sources of energy in the market. Given the harsh conditions, the overall process of harvesting energy from ocean waves is challenging. This requires additional resources for the research and development of WECs. In addition to this, given the difficulty with service and maintenance of the system once deployed in the ocean, it is difficult to reduce the levelized cost of energy [5].

Wave energy harvesters are categorised as: oscillating water columns, wave activated bodies and overtopping

Sponsor and financial support acknowledgement: The Swedish Energy Agency is acknowledged for financial support, and this work has been conducted within the project P-42244-2

Rimmie Duraisamy is currently doing her PhD in 'Challenges in developing a Durable Wave Energy Transmission' in the Machine Design Department at KTH, Royal Institute of Technology, Stockholm 114 28, Sweden (e-mail: rimmie@kth.se).

Kjell Andersson is a Professor in the Machine Design Department at KTH, Royal Institute of Technology, Stockholm 114 28, Sweden (e-mail: kan@kth.se).

Digital Object Identifier: https://doi.org/10.36688/ewtec-2023-267

devices [6]. Most of these harvesters generate peak power when the frequency of incident waves coincide with the frequency of the device [1]. Point absorbers are compact WECs with buoys that are actuated through hydrodynamic wave forces. In most cases, these buoys are connected to a linear actuator power take – off (PTO) system [7]. These linear systems have a finite stroke length and undergo huge end stop forces during storms that are often larger than the damping force provided by the PTO [8]. To overcome these limitations, KTH is developing a winch based point absorber wave energy converter, WBPA-WEC where a chain is wound around a drum to replace the linear actuators. Fig. 1 shows a schematic of the 'Lifesaver' winch based point absorber system developed by Fred Olsen [9]. The pre tensioner maintains the tension in the system at its reference state. The winch is connected to the PTO system, which translates wave motion into electricity.

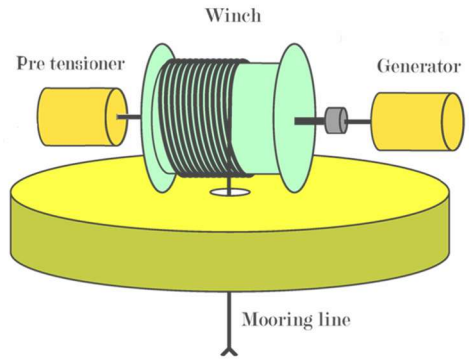

Fig. 1: Fred Olsen WBPA system [9]

A chain, if correctly dimensioned can withstand large tensile forces and can eliminate bending forces when its wound and unwound around the drum. When winding the chain around the drum, the bearings in the link undergo repetitive rolling and sliding. With elastomer elements in the bearings, this rolling and sliding is eliminated and the motion is realised as deformation of the elastomer. This reduces the risk of bending fatigue failure of the chain as well as increases the durability of the chain link [5]. Fig. 2 shows the preliminary design of the elastomer bearing in the chain link arrangement. Andersson et al have discussed the design process of the chain link in detail in [5].

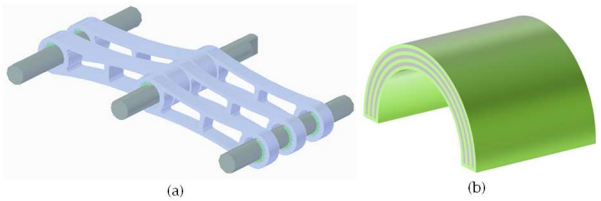

Fig. 2: (a) 2+3 Chain link configuration, (b) Elastomer bearing [5]

Since elastomers are non-linear, under large deformations, the classical theory for small deformations can no longer describe its properties adequately. Continuum mechanics is required to model these large deformations [10]. Many hyperelastic constitutive models have been proposed over the years some of which include neo-Hookean, Mooney-Rivlin [11], Arruda & Boyce [12], Yeoh [13] and Ogden [14]. The application of these models largely depend on the deformation mode and the deformation range of the elastomer.

In this application, the winch sub-system is designed in such a way that the elastomer bearing does not undergo more than 20% - 30% compression and 10° angular deformation when it rolls and unrolls around the drum [5]. However, the operating range does not exceed 5° angular displacement as described in Fig. 3. Given the choice of the shape factor for the bearing, any excess compression would lead to shear hardening. In this paper, an effort is made to identify the material parameters for two different elastomers.

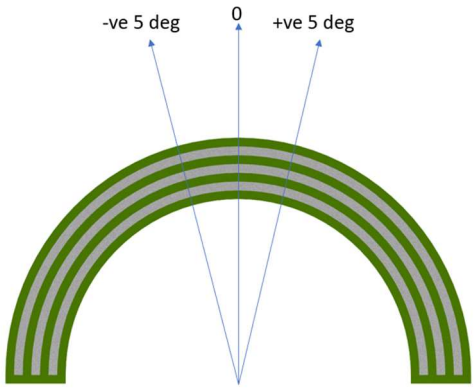

Fig. 3: Angular deformation of the elastomer bearing

II. METHODOLOGY

A design process for development of wave energy converters (WEC) has been presented in [15]. The work presented in this paper can be considered as one of the outlined activities in the detail design phase for a winch based wave energy converter, WB-WEC. This section describes the systematic process, see Fig. 4, for obtaining the material properties of an elastomer required for FE modelling and analysis. A verified material model can be used for designing and predicting the properties of the elastomer bearing. Main activities in this process are the material tests, followed by curve fitting to identify material model parameters and verification of these parameters using finite element analysis. The preliminary design of the bearing as shown in Table 1 is obtained using the bearing design methodology described in Gent [16]. The bearing design calculation has been explained in detail by Andersson et al [5].

TABLE 1:
BEARING PROPERTIES

Bearing design data	Values
Mean radius	13.5 [mm]
No. of elastomer layers	3
Thickness of the elastomer layers	1 [mm]
Compressive stiffness, K_c	12500 [N/mm]
Shear stiffness, K_s	1350 [N/mm]
No. of steel shims	2
Thickness of the steel shims	1 [mm]

Fig. 4 shows a systematic approach for obtaining the material parameters for the elastomer elements.

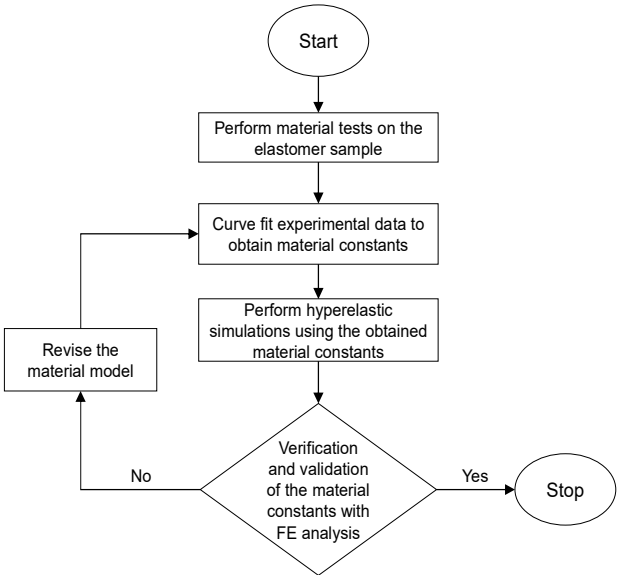

Fig. 4: Systematic design approach for determination of elastomer material properties

A. *Test Set up*

This study focuses on two different elastomer elements: Silicone and Polyurethane with hardness Shore 80A. Two different materials with the same hardness are selected to understand and compare the differences between them. Elastomer ring of inner diameter 23 mm and outer diameter 25 mm with 1 mm in thickness is used as a test sample. Fig. 5 shows the schematic of the test sample. Since the elastomer layers in the bearing are dimensioned to 1 mm thickness, the same is used for material tests. The width of the elastomer ring is 2 mm in order to obtain uniform shear across the sample width.

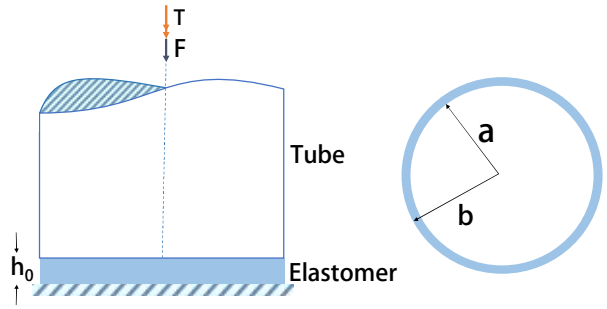

Fig. 5: Loading of the test sample with a = 23 mm, b = 25 mm and h0 = 1 mm

The MTS 809 axial/torsion machine, with force capacity of 250 kN and torque capacity of 2200 Nm is used to conduct the tests [17]. One end of the elastomer sample is glued to the steel plate and the other end to a hollow steel tube. Fig. 6 shows the test set up. Since in the application, the bearing undergoes compression and shear consecutively, the material tests are designed to replicate a similar load case.

The silicone test sample is subjected to 50% compression followed by 1° of shear; while, the polyurethane sample is subjected to 40% compression followed by 0.5° of shear. The samples are compressed at the rate of 0.01 mm/s and held constant for 30 seconds. The compressed samples are then subjected to angular deformation at the rate of 0.01 °/s. The reaction force and reaction moment are recorded.

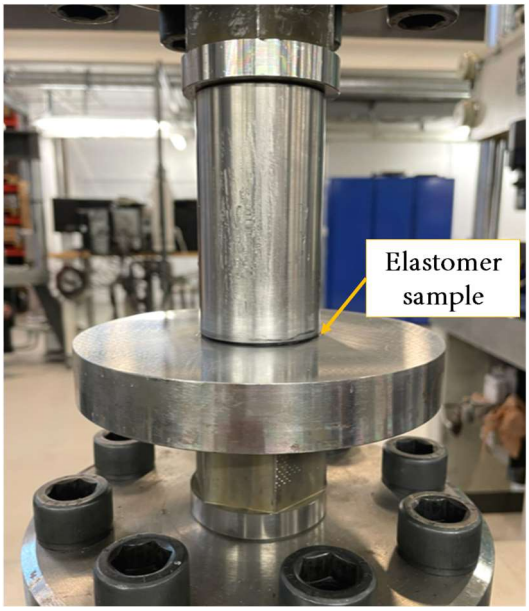

Fig. 6: Test set up of the elastomer ring

The tests are repeated in order to account for the softening of elastomer due to Mullins Effect. Fig. 7 and Fig. 8 show the test data for Silicone 80A and PU 80A respectively. Note, despite the same hardness of Shore 80A for silicone and PU, silicone is much softer than polyurethane.

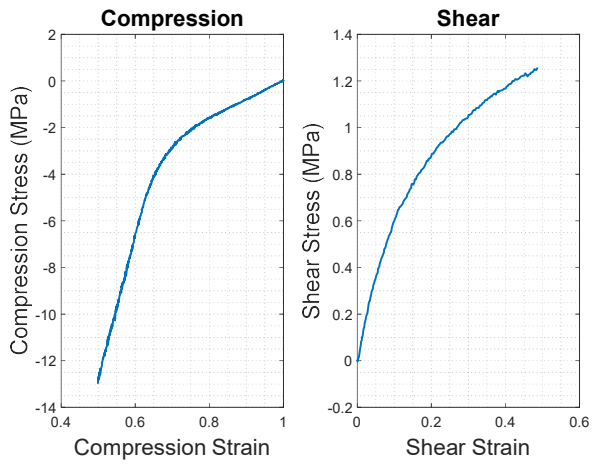

Fig. 7: Experimental data for Silicone

The compression strain affects the shear modulus [16]. As seen from the experimental data in Fig. 7 and Fig. 8, the materials exhibit a sudden increase in the compression stiffness after 20% compression.

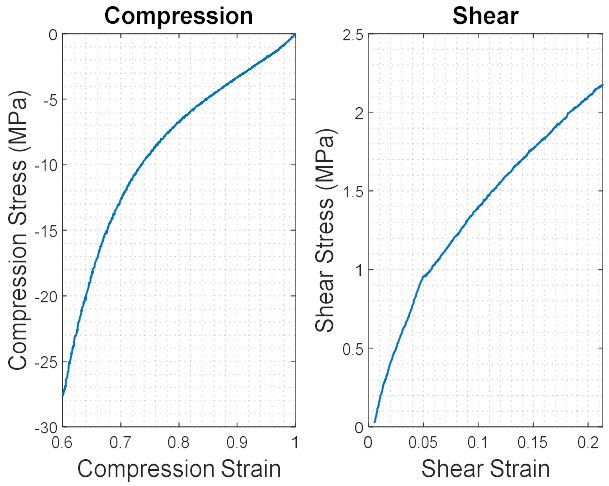

Fig. 8: Experimental data for Polyurethane

B. *Constitutive Modelling*

Here, incompressible hyperelastic material models are considered for curve fitting. Since only Mooney-Rivlin and Yeoh models are used in this study, the discussion is limited to these models.

The strain energy function for Mooney-Rivlin is given as [18, 19]:

$$\psi = \sum_{i=0,j=0}^{n} C_{ij}(I_1-3)^i(I_2-3)^j \tag{1}$$

Where I_1 and I_2 are the invariants, C_{ij} is the material parameter to be determined given $C_{00}=0$ and n is the number of terms.

The Yeoh strain energy function is written as [18, 19]:

$$\psi = \sum_{i=1}^{n} C_i(I_1-3)^i \tag{2}$$

C_i is the material parameter and

In terms of principal stretches λ_1, λ_2 and λ_3,

$$I_1 = \lambda_1^{\,2} + \lambda_2^{\,2} + \lambda_3^{\,2} \tag{3}$$

$$I_2 = \lambda_1^{\,-2} + \lambda_2^{\,-2} + \lambda_3^{\,-2} \tag{4}$$

Equation (5) gives the relation between engineering stress and the strain energy function

$$\sigma = F\frac{\partial \psi_{iso}}{\partial C}F^T - \kappa I \tag{5}$$

Where, ψ_{iso} is the isochoric part of the strain energy function, C is the Right Cauchy Green Strain given as $C = F^T F$ and F is the deformation gradient.

Since the elastomer undergoes both compression and shear consecutively, the deformation gradient is calculated as:

$$F = \begin{pmatrix} \lambda & 0 & 0 \\ \gamma & 1 & 0 \\ 0 & 0 & \frac{1}{\lambda} \end{pmatrix} \tag{6}$$

λ and γ represent stretch in compression and shear strain respectively.

Equations (7) and (8) show the analytical engineering stress for 2 parameter Mooney-Rivlin model.

$$\sigma_{11} = 2(C_1+C_2)(\lambda^2 - \frac{1}{\lambda^2}) - C_1\gamma^2 \tag{7}$$

$$\sigma_{21} = 2\gamma(\lambda C_1 + \frac{C_2}{\lambda}) \tag{8}$$

C_1 and C_2 are the material parameters to be determined.

The calculated engineering stress for Yeoh model are represented in equations (9) and (10).

$$\sigma_{11} = 2iC_i(\lambda^2 - \frac{1}{\lambda^2})(\lambda^2 + \frac{1}{\lambda^2} - 2)^{(i-1)} \tag{9}$$

$$\sigma_{21} = 2iC_i\lambda(\gamma^3 - 0.53\gamma)^{(i-1)} \tag{10}$$

C_i denotes the material parameter.

σ_{11} represents the stress in compression while σ_{21} represents the shear stress.

C. *Determination of the Material Parameters*

Curve fit aims to predict the parameters such that the model function is approximated as closely as possible with the experimental data [18]. In this study, it is achieved using the optimization function in MATLAB where, the objective function is minimized. The objective function in

this application comprises of the compression and shear load case. Regression analysis is used to minimize the objective function as shown in equation (11).

$$\in = \sum_{i,j=1}^{n} (\sigma_E(\lambda) - \sigma(\lambda_i, \gamma, C_{ij}))^2 \rightarrow \min \quad (11)$$

Where, $\in$: total error to be minimized

σ_E : engineering stress from the experimental data

i, j : number of data pairs

The error is a combination of error from the compression data and the shear curve fit, see equation (12).

$$\in = \in_c + \in_s \quad (12)$$

$\in_c$: error from compression curve fitting

$\in_s$: error from shear curve fitting

The accuracy of curve fit is evaluated using the coefficient of determination as shown in equation (14) [20]. Equation (13) is the adjusted coefficient of determination where it accounts for the number of parameters in the material model function. For a good fit, the value of equation (13) must be closer to 1.

$$\overline{R^2} = 1 - \frac{n-1}{n-p-1}(R^2 - 1) \quad (13)$$

$$R^2 = 1 - \frac{\sum_{i=1}^{n}(Y_i - \hat{Y}_i)^2}{\sum_{i=1}^{n}(Y_i - \overline{Y}_i)^2} \quad (14)$$

Where, n : no. of data pairs

p : no. of parameters in the material model function

Y_i : Experimental values

$\hat{Y}_i$: Predicted values in the material model function

$\overline{Y}_i$: Average of experimental values

D. *Finite Element Method Verification of Material Parameters*

The material parameters obtained from curve-fit are further verified using finite element (FE) analysis in COMSOL.

A three dimensional quasi-static simulation is set up where the elastomer sample is subjected to gradual compression followed by shear. Similar to the experimental set up, the reaction force and torsion is recorded as output.

III. RESULTS

The material parameters obtained from curve fitting for Silicone is shown in Table 2. Mooney-Rivlin 2 parameter model turned out to give the best fit.

TABLE 2:
MATERIAL PARAMETERS FOR SILICONE

Material Parameters for Silicone 80A	
Material Model	Mooney-Rilvin 2 parameters
C_1	0.038166 [MPa]
C_2	0.78827 [MPa]
Bulk modulus	8e6 [Pa]

However, from Fig. 9, it can be observed that the initial compressive stiffness is underestimated in the finite element simulation and the compression stress varies by 20% while it is overestimated in the numerical curve fitting performed using the analytical equations and the stress varies by 40% compared to the measurements. Further, the shear data has a very poor curve fit. At 0.5° of shear, which corresponds to the value 0.2 in shear strain, the difference between measured and estimated shear stress is 40%. Gradually, after 0.8°, both, the FE model and the analytical model overestimate the shear stiffness.

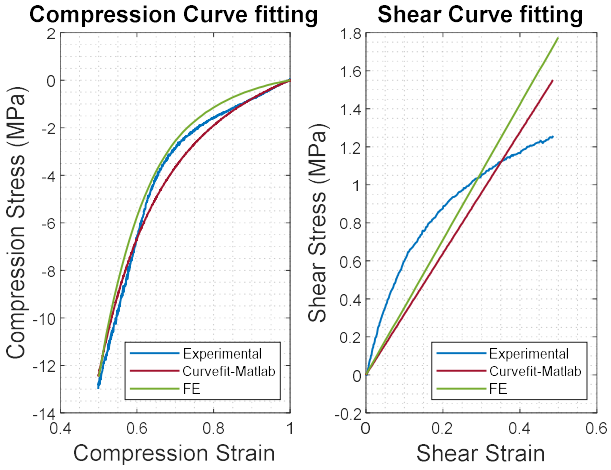

Fig. 9: Curve fit for Silicone

Yeoh 3 parameter model was the best fit for polyurethane as shown in Table 3.

A bulk modulus of 3.4e8 Pa was assumed in finite element simulations while, the numerical curve fitting using analytical calculations assumed the material as incompressible.

TABLE 3:
MATERIAL PARAMETERS FOR POLYURETHANE

Material Parameters for PU 80A	
Material Model	Yeoh 3 parameters
C_1	4.6085 [MPa]
C_2	-1.4471 [MPa]
C_3	0.87097 [MPa]
Bulk modulus	3.4e8 [Pa]

Fig. 10 shows the curve fitting for polyurethane. Note that similar curve fit behaviour is noticed here. The initial compressive stiffness is underestimated in the finite

element simulation and the compression stress varies by 50% as compared to the measured data.

The shear stiffness is overestimated at 0.3° and 0.4° of shear by FE model and analytical model respectively. At 0.5°, as compared to the measurements, the analytical model differs by 12.5% and FE model by 37.5%.

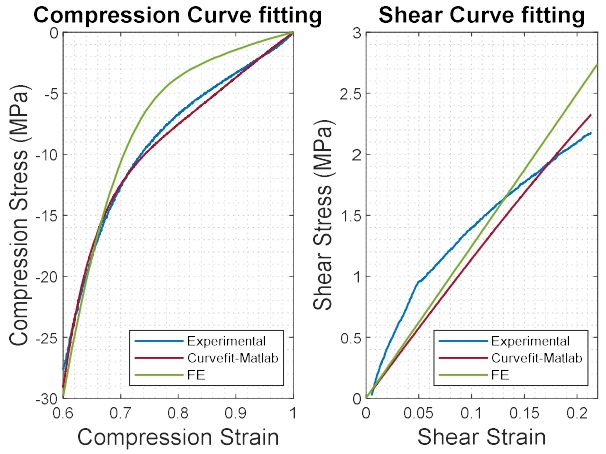

Fig. 10: Curve fit for Polyurethane

IV. Discussion

There are many possible reasons for the large differences identified in Fig. 9 and Fig. 10. As discussed previously, the behaviour of an elastomer changes with its loading conditions. In this study, no standard test procedure is followed for determining the material properties of the elastomer. The test conditions are curated to best adapt to the load conditions in the actual application. Since, the test samples were glued on both ends, constrained compression is induced in the sample. Moreover, the test samples being used were only 2 mm wide. This can increase the possibility of uneven stress distribution throughout the sample.

When developing the analytical equations, it was assumed that the elastomer is incompressible. However, in the finite element simulations, the material resulted in a significantly stiff behaviour when incompressible boundary condition was implemented. Hence, as mentioned in Table 2 and Table 3, a nearly incompressible boundary condition was introduced in the simulations by assigning a bulk modulus to the material model.

These assumptions explain the differences between the results obtained from analytical curve fitting and FE simulations.

In addition to this, from Fig. 9 and Fig. 10, it can be observed that there exists tension-compression asymmetry in the elastomer test samples. This explains the linear curve fit for shear load case. However, Ricker et al [21] argue that material models dependent on I_2 invariant can provide better fit for curves with concave behaviours, in this case, the shear data.

V. Conclusion

A wave energy converter is a complex system that consists of many systems and sub-systems, which require to be designed for harsh marine environment involving many uncertainties. This makes the design and development of WEC a challenging process. A systematic design process can simplify and streamline the development process. It divides the system into a set functions and sub functions by emphasizing on the requirements [15].

An outline of the WEC designing process has been discussed in detail in [15]. A WBPA-WEC is divided into different functions where the development of a winch system fall under the mechanical function structure. This article is a continuation of the winch development system done by Andersson et al [5].

In this paper, a systematic design process has been suggested to evaluate and determine the material parameters for an elastomer element undergoing compression and shear.

This will enable the development of an elastomer bearing for a WBPA-WEC being researched and developed at KTH. The discussion to determine the material properties of the elastomer illustrate the different steps of the design process in Fig. 4.

The results and discussions above indicate that the material model must be revised with more suitable material parameters that can provide a better curve fit for the elastomer test data. This includes investigating into material models with dependency on I_2 invariant and in which the tension-compression asymmetry can be adjusted and modified.

The suggested process model for material characterization has been illustrated for two hyperelastic materials and we can conclude that it can facilitate the development of material models of these type of materials.

VI. Future Work

The next step in the development of the winch concept includes evaluation of the drum and the design of the chain link. Stiffness measurements are ongoing to evaluate the bearing design. However, reliable finite element model of the bearing can enable a faster evaluation of the design and assist with design modifications along with its verification and validation.

An accurate material model of an elastomer element is crucial to this. The current material model results in large differences with the existing bearing tests. Following further investigation and development of an accurate material model, the future work involves developing a reliable bearing design and a winch system that can fulfil the requirements for a functioning wave energy converter.

Acknowledgement

The authors of this article would like to thank T. Christian Gasser and Martin Öberg at the Solid Mechanics

department, KTH, for their expert guidance in the subject and help with the material tests.

REFERENCES

[1]. Drew, B., A.R. Plummer, and M.N. Sahinkaya, *"A review of wave energy converter technology."* Proceedings of the Institution of Mechanical Engineers, Part A: Journal of Power and Energy, 2016. **223**(8): p. 887-902.

[2]. Ross, D., *"Power from the Waves."* 1995: Oxford University Press, USA.

[3]. Falcão, A.F.d.O., *"Wave energy utilization: A review of the technologies."* Renewable and Sustainable Energy Reviews, 2010. **14**(3): p. 899-918.

[4]. Waters, R., *"Energy from Ocean Waves Full Scale Experimental Verification of a Wave Energy Converter."* 2008, Uppsala University.

[5]. Andersson, K., A. Hagnestål, and U. Sellgren, *"A Flexible Chain Proposal for Winch-Based Point Absorbers."* Journal of Mechanical Design, 2019. **141**(10).

[6]. Salter, S.H., *"Wave power."* Nature, 1974. **249**(5459): p. 720-724.

[7]. Ulvgård, L., et al., *"Line Force and Damping at Full and Partial Stator Overlap in a Linear Generator for Wave Power."* Journal of Marine Science and Engineering, 2016. **4**(4): p. 81.

[8]. Brekken, T., B. Batten, and E.A. Amon, *"From Blue to Green [Ask the Experts]."* Control Systems, IEEE, 2011. **31**: p. 18-24.

[9]. Sjolte, J., et al., *"Exploring the Potential for Increased Production from the Wave Energy Converter Lifesaver by Reactive Control."* Energies, 2013. **6**(8): p. 3706-3733.

[10]. Gajewski, M., R. Szczerba, and S. Jemioło, *"Modelling of Elastomeric Bearings with Application of Yeoh Hyperelastic Material Model."* Procedia Engineering, 2015. **111**: p. 220-227.

[11]. Mooney, M., *"A Theory of Large Elastic Deformation."* Journal of Applied Physics, 2004. **11**(9): p. 582-592.

[12]. Boyce, M.C. and E.M. Arruda, *"Constitutive Models of Rubber Elasticity: A Review."* Rubber Chemistry and Technology, 2000. **73**(3): p. 504-523.

[13]. Yeoh, O.H., *"Characterization of Elastic Properties of Carbon-Black-Filled Rubber Vulcanizates."* Rubber Chemistry and Technology, 1990. **63**(5): p. 792-805.

[14]. Ogden, R.W., *"Non-linear Elastic Deformations."* 1984: E. Horwood.

[15]. Rimmie Duraisamy, Kjell Andersson., *" Outlining a Design Process for a Winch- Based Point Absorber Wave Energy Converter."* in *NordDesign 2022*. 2022.

[16]. Gent, A.N., *"Engineering with Rubber- How to Design Rubber Components."* Third ed. 2012, Munich: Hanser Publishers.

[17]. Systems, M.; Available from: https://www.mts.com/en/products/materials/dynamic-materials-test-systems/series-809-at-test-systems.

[18]. Rackl, M. *"Curve Fitting for Ogden, Yeoh and Polynomial Models."* 2015.

[19]. Gasser, T.C., *"Vascular Biomechanics."* 2021.

[20]. Fahrmeir, L., et al., *"Regression: Models, Methods and Applications."* 2013.

[21]. Ricker, A. and P. Wriggers, *"Systematic Fitting and Comparison of Hyperelastic Continuum Models for Elastomers."* Archives of Computational Methods in Engineering, 2023.